

First-principles study of the mechanisms for the pressure-induced phase transitions in zinc-blende CuBr and CuI

Yanming Ma,* John S. Tse, and Dennis D. Klug

Steacie Institute for Molecular Sciences, National Research Council of Canada, Ottawa, Ontario K1A 0R6, Canada

(Received 12 September 2003; published 11 February 2004)

The lattice dynamics of zinc-blende (ZB) CuBr and CuI is studied as a function of pressure using density functional linear-response theory. A pressure-induced soft transverse acoustic (TA) phonon mode is identified for both compounds. Each compound shows a different pressure-induced phonon softening behavior. A TA phonon branch softens along the $[\xi\xi 0]$ direction in CuBr, resulting in a phase transition from a ZB phase (CuBr-III) to a tetragonal phase (CuBr-IV). A softening TA phonon mode at the zone boundary L point in CuI may induce a phase transition from a ZB phase (CuI-III) to a rhombohedral phase (CuI-IV), although the phonon softening towards zero frequency in CuI is superseded by a first order phase transition occurring at 1.74 GPa. Possible phase transition paths are presented for both compounds.

DOI: 10.1103/PhysRevB.69.064102

PACS number(s): 64.70.Kb, 63.20.Dj, 62.50.+p, 31.15.Ar

Copper halides (CuCl, CuBr, CuI) are the most ionic crystals with a zinc-blende (ZB) lattice structure. Their ionicities approach the critical threshold at which the ZB structure becomes unstable with respect to the more closely packed NaCl or CsCl structure, due to the electrostatic interactions.¹ As a result of this near structural instability, a large number of pressure-induced polymorphs are possible. The available experimental evidence²⁻⁵ suggests that all three copper halides adopt a rocksalt structure at pressures in the region of ~ 10 GPa. In addition, these copper halides undergo a number of structural phase transitions under pressure before attaining the rocksalt structure. It is known that upon application of pressure, ZB CuCl (CuCl-II) first transforms to an unknown intermediate phase CuCl-IIa, then goes to a cubic phase (CuCl-IV); ZB CuBr (CuBr-III) goes to a tetragonal phase (CuBr-IV); and ZB CuI (CuI-III) transforms to a rhombohedral phase (CuI-IV). The three copper halides crystallize in the same ZB phase with similar bonding behaviors at normal conditions. In this study, we examine why they each transform from the ZB structure to different structures under pressure.

Dynamic instabilities are often responsible for phase transitions under pressure.⁶ Lattice dynamics plays an important role in understanding the different mechanisms of phase transitions in the same type of compounds. A detailed study of the phonon spectra with pressure in cesium halides reveals the different mechanisms of phase transitions in CsI, CsBr, and CsCl.⁷ In our previous work,⁸ a mechanism driving the phase transition from CuCl-II to CuCl-IV was revealed by the *ab initio* calculation of the transverse acoustic (TA) phonon softening at the zone boundary X point of the first Brillouin zone. Moreover, there are very large mean-square vibrational amplitudes for Cu, Cl, Br, and I ions in the three copper halides,⁵ which are related to the lattice dynamics. In addition, the differences in the three compounds are the mass and ionic radii differences, which also determine the details of the dynamics. To probe the difference in the mechanisms of the phase transitions in the three copper halides, further detailed *ab initio* calculations of the lattice dynamics for

CuBr and CuI are, therefore, motivated. This study contributes to the understanding of the mechanisms of pressure-induced phase transitions in copper halides.

The lattice dynamics for both compounds is investigated using the pseudopotential plane-wave density-functional linear-response method.⁹ The generalized gradient approximation (GGA) of the exchange-correlation functional is employed.¹⁰ The Troullier-Martins¹¹ norm-conserving scheme is used to generate the pseudopotentials for Cu, Br, and I, respectively. The kinetic energy cutoff, E_{cutoff} , was chosen as 90 Ry for both CuBr and CuI, respectively, to ensure the convergence of the calculated phonon frequencies to within 0.02 THz. A $4 \times 4 \times 4$ k mesh in the first Brillouin zone was used in the phonon calculations. The theoretical equilibrium lattice constants are determined by fitting the total energies as a function of volume to the Murnaghan¹² equation of state. Table I shows the calculated values for equilibrium lattice parameters and bulk moduli, along with another theoretical calculation¹³ and the experimental measured results,^{5,14} which can be used to estimate both the accuracy of our pseudopotentials and the GGA approximation for the studied systems. It is known that the bulk modulus in copper halides decreases with increasing temperature.¹³ As a reference, the bulk moduli for CuCl measured at 4.5 and 300

TABLE I. Calculated equilibrium lattice parameter (a_0), bulk modulus (B_0), and the pressure derivative of bulk modulus (B'_0) for the zinc-blende CuBr and CuI. Another theoretical calculation from Ref. 13 and experimental results from Refs. 5 and 14 are also shown for comparison in parentheses. The units for a_0 and B_0 are in Å and Mbar, respectively.

	a_0 (Å)	B_0 (Mbar)	B'_0
CuBr	5.70{5.70 ^a }(5.63 ^b)	0.48{0.37 ^a 0.44 ^c }(0.54 ^b)	4.98 (3.70 ^b)
CuI	6.09{6.05 ^a }(6.01 ^b)	0.47{0.37 ^a }(0.48 ^b)	4.90 (8.00 ^b)

^aExperimental data at room temperature taken from Ref. 5.^bTheoretical results taken from Ref. 13.^cExperimental data at $T=77$ K taken from Ref. 14.

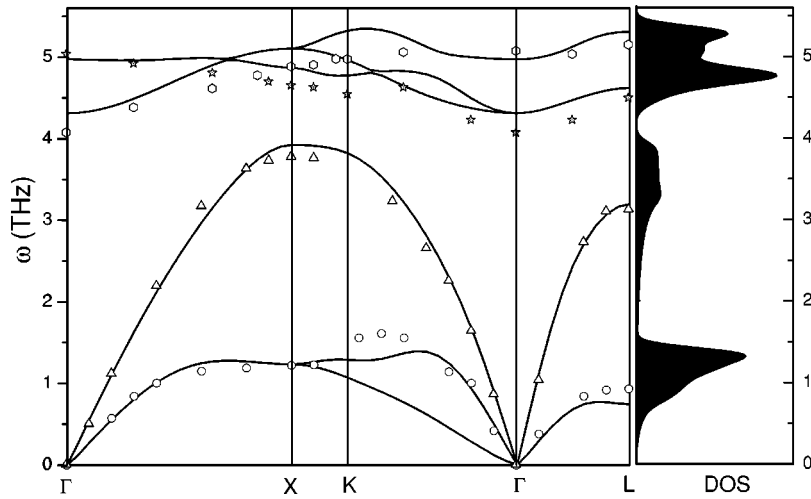


FIG. 1. The calculated phonon frequencies (solid lines) and density of states (DOS) of zinc-blende CuBr at zero temperature, along with the experimental phonon dispersion data (symbols) at $T = 77$ K (Ref. 18).

TABLE II. Calculated phonon frequencies for CuBr and CuI at high symmetry points of the Brillouin zone. Values in parentheses are the results for another *ab initio* calculation taken from Ref. 16. The experimental data shown in curly brackets are taken from Refs. 15 and 19 for CuBr and CuI, respectively. The unit for frequencies is THz.

	K points	TA	LA	TO	LO
CuBr	Γ			4.31 (4.02){4.05}	4.97 (4.74){5.07}
	X	1.23 (1.53){1.17}	3.92 (3.72){3.78}	5.11 (4.74){4.83}	4.87 (4.71){4.62}
	L	0.75 (1.26){0.96}	3.20 (3.39){3.18}	5.31 (5.01){5.16}	4.62 (4.35){4.50}
CuI	Γ			4.39 (3.48){3.78}	4.80 (3.96){4.80}
	X	1.49 (1.71){1.38}	3.93 (3.45){3.63}	4.66 (3.63){4.29}	4.10 (3.54){4.67}
	L	1.18 (1.26){1.08}	3.27 (3.18){3.00}	4.60 (3.72){4.65}	4.48 (3.54){3.99}

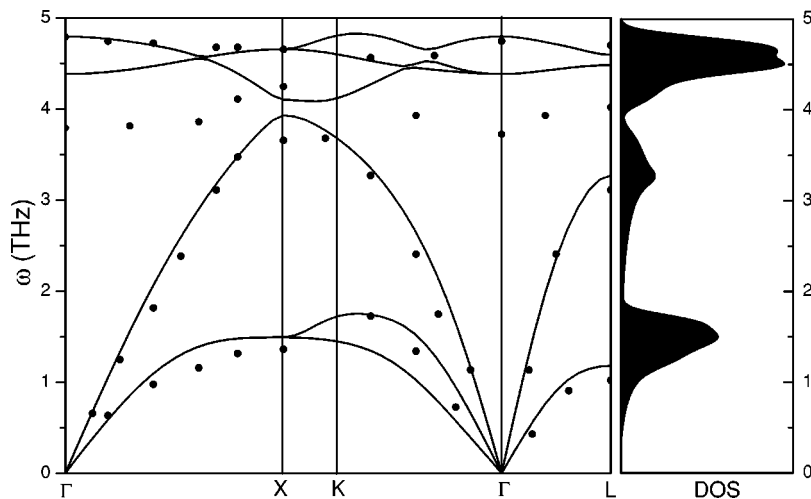


FIG. 2. The calculated phonon frequencies (solid lines) and DOS of zinc-blende CuI at zero temperature, together with the experimental phonon dispersion data (symbols) at $T = 300$ K (Ref. 19).

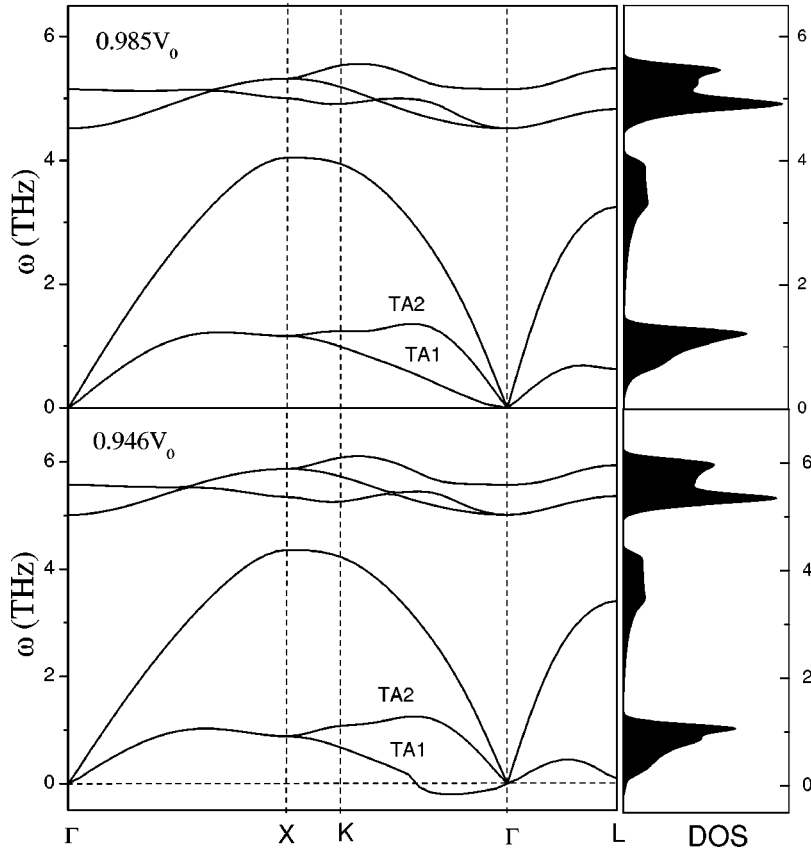


FIG. 3. Calculated phonon frequencies and DOS of zinc-blende CuBr at different volumes.

K are 0.65 (Ref. 15) and 0.38 Mbar,⁵ respectively. The calculated equilibrium lattice constants for both compounds are used to study the phonon dispersion curves at zero pressure.

For ZB CuCl, our *ab initio* calculation on phonon dispersion successfully reproduced the experimental results at zero pressure and at extremely low temperature $T=4.2$ K.⁸ Few *ab initio* phonon calculations in CuBr and CuI are reported in the literature. Recently, Serrano *et al.*¹⁶ presented their *ab initio* phonon results for CuBr and CuI at Γ , X , and L points of the Brillouin zone. To compare with the inelastic neutron experimental results, *ab initio* calculations for the phonon dispersion curves in CuBr and CuI were still not available. Figure 1 shows the comparison of our *ab initio* phonon dispersion curve at zero temperature with the experiment at $T=77$ K in ZB CuBr.¹⁵ The agreement between theory and experimental data is satisfactory. Note also that the calculated phonon density of states (DOS) agrees well with that of a shell-model calculation.¹⁷ The temperature has noticeable

TABLE III. The calculated elastic constants for ZB CuBr in GPa units. The available experimental data taken from Ref. 15 at $T=293$ K are indicated in parentheses.

	V_0	$0.984V_0$	$0.946V_0$
C_{11}	42.9 (43.4)	47.8	51.9
C_{12}	31.7 (33.2)	43.8	53.1
C_{44}	13.9 (14.3)	13.2	11.6
C_s	5.6 (5.1)	2.0	-0.6

negative frequency shift effects on the phonons in copper halides.^{15,18} The discrepancy between theory and experiment in optical modes mainly results from the temperature-induced shift of phonon frequencies. It should be pointed out that our *ab initio* calculation successfully reproduces the phonon line shape with a crossing feature near the X point. Table II lists the comparison between our *ab initio* calculation and Serrano *et al.*'s work,¹⁶ together with the experimental data for CuBr at Γ , X , and L points, respectively. The current calculation shows a better agreement with the experimental results.

Figure 2 presents our *ab initio* phonon dispersion curve and one-phonon DOS at zero temperature, along with the experimental data from Hennion *et al.*¹⁹ at $T=300$ K in ZB CuI. The comparison of our *ab initio* calculation with Serrano *et al.*'s¹⁶ work for CuI at Γ , X , and L points is also listed in Table II. The agreement between this calculation and experimental data is very good for transverse acoustic phonon modes. However, for optical phonon modes, the agreement is not as satisfactory. Our theoretical phonon dispersion clearly shows an anomalous crossing feature between the transverse optical (TO) branch and the longitudinal optical (LO) branch near the X point, similar to the results of CuBr at low temperature. The available experimental phonon dispersion in ZB CuI at room temperature, however, does not show a similar crossing behavior. To understand the discrepancy resulting from the temperature difference between the theoretical calculation and experimental results, several aspects should be addressed. First, for CuBr, as a reference

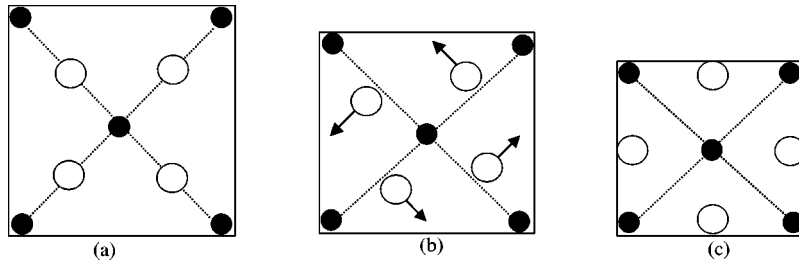


FIG. 4. A schematic representation for the possible transition path in CuBr from the ZB phase to the tetragonal phase. (a) A top view of 001 plane in a unit cell of the ZB phase. There are five Cu atoms in one plane shown as solid circle. Four Br atoms in adjacent layers along the diagonals are shown by the open circle. The atomic displacements of Br atoms are along $[1\bar{1}0]$, i.e., perpendicular to the $[110]$ direction. The arrows show the projection in the 001 plane of the displacements for Br atoms as indicated in (b). A new tetragonal phase is formed when Br atoms reach the face of the edge, as illustrated in (c).

system, the measured phonon dispersion curve by Prevot *et al.*²⁰ does not show a crossing feature between TO and LO phonon branches near the X point at room temperature, while the phonons measured by Hoshino *et al.*¹⁵ do show a crossing feature at $T=77$ K. Second, the phonon frequency for TO (X) is larger than that of LO (X) in another *ab initio* calculation,¹⁶ as shown in Table II, directly supporting the crossing feature of phonon dispersion near the X point in our *ab initio* calculation. Third, the interionic forces of CuBr and CuI exhibit a complex behavior due to the mixture of covalent and ionic bonding. With increasing temperature, the significant thermal-anharmonic effects may contribute to the changes of the line shape of phonon dispersion. Finally, for some metals, such as Hf, La, Ti, and Sc, this crossing anomaly is also seen at low temperature but vanishes at high temperatures,²¹ similar to our results. Therefore, the anomalous crossing between TO and LO phonon branches is the main feature of the phonon dispersions of CuBr and CuI at low temperature, as supported by our *ab initio* calculation, while the absence of phonon band crossing apparently de-

scribes the behavior of phonon dispersion at high temperature.

The calculated phonon dispersion curves of CuBr and the one-phonon DOS at different volumes are shown in Fig. 3. With decreasing volume, the TO, LO, and longitudinal acoustic (LA) phonon modes shift to higher frequencies, while the whole TA phonon branch decreases in frequency, indicating a negative mode Grüneisen parameter, $\gamma_j(q) = -\partial \ln \omega_j(q) / \partial \ln V$ for mode j , where q is wave vector, ω is the frequency, and V is the volume. At a volume of $0.946V_0$, the phonon frequencies of the TA modes along the $[\xi\xi 0]$ branch (labeled by TA1) become imaginary, signaling a structural instability in the zinc-blende phase of copper bromide. The estimated transition pressure from CuBr-III to CuBr-IV is ~ 3.0 GPa ($V=0.946V_0$) which is somewhat less than the experimental transition pressure (~ 4.85 GPa) at $T=300$ K.⁵ The origin of this difference may be attributed to the neglect of temperature effects, which are expected to be significant. The elastic constants of ZB CuBr with volume are shown in Table III, as calculated from the slopes of the

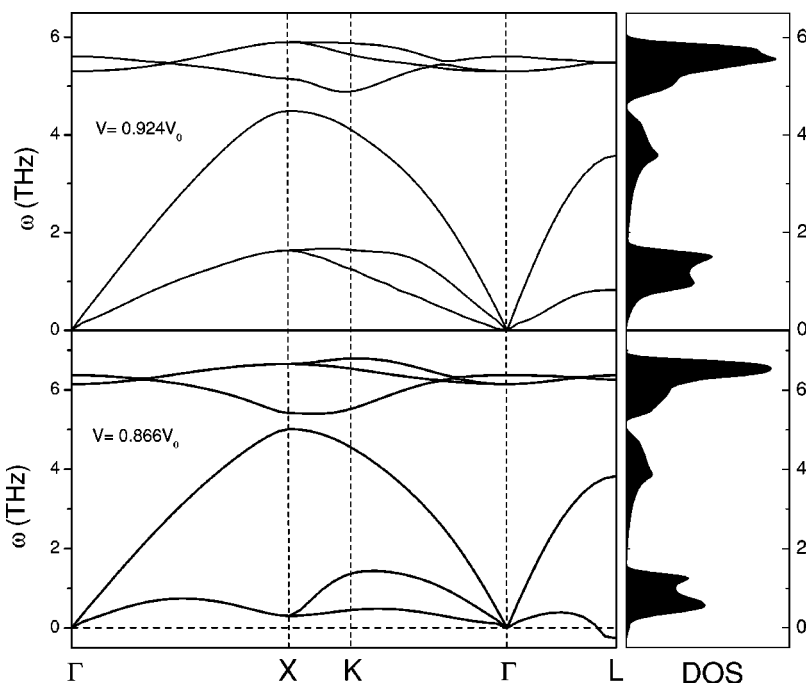


FIG. 5. Calculated phonon frequencies and DOS of zinc-blende CuI at different volumes.

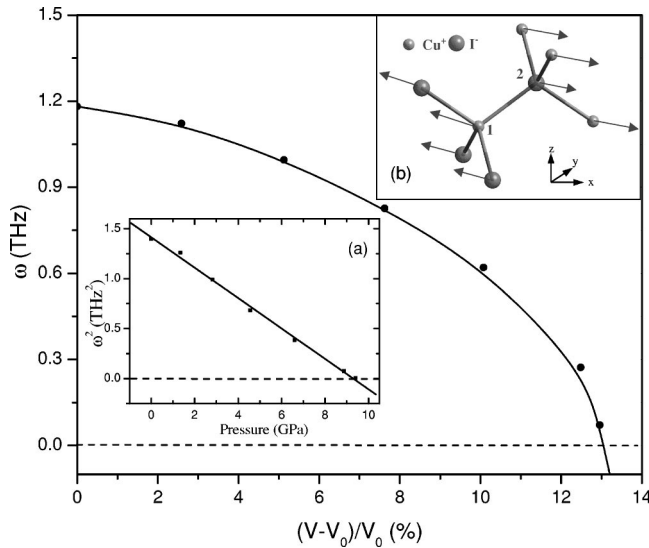


FIG. 6. Main figure: Calculated TA (L) frequencies in CuI as a function of volume. The solid line through the calculated data points represents fitted curves using a B spline. Inset: (a) The calculated squared phonon frequency ω^2 as a function of pressure; the solid line through the data points is a linear fit. (b) The eigenvector for TA phonon mode at the L point. Atom 1 is a Cu atom at (0 0 0). The other three Cu atoms are at (0 1/2 1/2), (1/2 1/2 0), and (1/2 0 1/2), respectively. Atom 2 is the I atom at (1/4 1/4 1/4). The other three I atoms are at $(-1/4 -1/4 1/4)$, $(1/4 -1/4 -1/4)$, and $(-1/4 1/4 -1/4)$, respectively. The arrows show the directions of atomic displacement. The direction from atom 1 to atom 2 is [111].

phonon dispersion curves at $q \rightarrow 0$.²² It is clear that C_s , the tetragonal shear elastic constant, $1/2(C_{11}-C_{12})$, manifested in the long-wavelength part of the transverse branch along $[\xi\xi 0]$ with the polarization vector along $[1\bar{1}0]$,^{21,23} becomes negative at $V=0.946V_0$, and this contributes to the phonon softening behavior of CuBr. This tetragonal shear distortion, physically, modifies the c axis, but keeps a and b axes the same, while conserving the volume.²⁴ A consequence of the instability of this shear modulus is a phase transition from cubic structure to a tetragonal structure. One possible transition path is presented in Fig. 4. A top view along the c axis of the three adjacent layers in ZB CuBr is shown in Fig. 4(a). As the C_s shear modulus becomes unstable with increasing pressure, lattice constants a and b decrease simultaneously, while the c axis length increases. The strain from the local distortion moves Br atoms out of the diagonal direction. The atomic displacements of Br atoms are along $[1\bar{1}0]$, i.e., perpendicular to the $[110]$ direction, as evidenced by the calculated eigenvectors (not shown) of the TA1 phonon branch along $[\xi\xi 0]$. The arrows show the projection in the 001 plane of the displacements for Br atoms, as indicated in Fig. 4(b). A new tetragonal phase is formed when Br atoms reach the face of the edge, as illustrated in Fig. 4(c). This physical picture shows how ZB CuBr transforms to a tetragonal structure under pressure in Fig. 4. This behavior is similar to that of the phase transition from a body centered cubic structure to a metastable tetragonal structure in the metallic elements Ti, Hf, and La.²¹

Figure 5 shows the variation of our theoretical phonon

dispersion curves and one-phonon DOS with pressure for ZB copper iodide. With increasing pressure, the TA phonon mode frequency at the zone boundary decreases, while other phonon modes shift to higher energy. At $V=0.866V_0$, the phonons soften to negative frequencies at the zone boundary L (0.5 0.5 0.5) point, indicating a possible structural instability. Figure 6 shows the variation of the TA mode with volume. The estimated volume for phonon softening to zero frequency from Fig. 6 is $\sim 0.869V_0$, corresponding to ~ 9.4 GPa. The squared phonon frequencies ω^2 for the TA branch at the L point with pressure P are also plotted, as shown in inset (a) of Fig. 6. A near perfect linear relation between ω^2 and P was obtained. Such a behavior is consistent with the Landau theory of pressure-induced soft mode phase transitions.²⁵ The calculated transition pressure, 9.4 GPa, is much higher than the experimental transition pressure, 1.74 GPa, at room temperature, even if one allows for the temperature effects. This big difference indicates that the phase transition from a ZB structure to a rhombohedral structure in CuI may not be induced independently by the phonon instability at the zone boundary L point. This behavior of the phonon softening to zero frequency is hidden by the first order transition to the rhombohedral phase. Although this phase transition occurs at pressures far below those required to drive the TA modes to zero frequency, the “mode-softening” behavior may be related to the particular mechanism that is responsible for the phase transition. The schematic representation of eigenvectors for the TA phonon mode at the L point is shown in inset (b) of Fig. 6. The Cu cation and I anion move perpendicular to the $[111]$ direction but in opposite directions, i.e., the Cu cation and I anion motions are polarized in the $[1\bar{1}\bar{1}]$ or $[\bar{1}11]$ directions, while the wave propagates along the $[111]$ direction. Phonon softening usually corresponds to the instability of a particular shear modulus. The ZB structure in CuI, therefore, tends to become unstable with respect to the atomic displacement perpendicular to the $[111]$ direction, which is responsible for the phonon softening at the L point, over all its domain of existence with no pretransitional effects occurring close to the first order transition. We remark that one possible physical driving mechanism for CuI from a ZB structure to a rhombohedral phase may be due to the instability of the shear behavior with atomic displacements perpendicular to $[111]$ direction.

In summary, the lattice dynamics of ZB CuBr and ZB CuI is studied as a function of pressure using density functional linear-response theory. A pressure-induced soft transverse acoustic (TA) phonon mode is identified for both compounds. Each compound shows a different pressure-induced phonon softening behavior. The TA phonon branch softens along $[\xi\xi 0]$ direction in CuBr, resulting in a phase transition from the ZB phase (CuBr-III) to a tetragonal phase (CuBr-IV). The mode softening behavior of the TA phonon at the zone boundary L point of the Brillouin zone in CuI may induce a phase transition from the ZB phase (CuI-III) to a rhombohedral phase (CuI-IV), although the phonon softening to zero frequency in CuI is hidden during the phase transition. Combining the current work with our previous study, the TA phonon mode softens at the zone boundary X point in

CuCl, initiating a phase transition from the ZB structure (CuCl-II) to a cubic structure (CuCl-IV).⁸ It is apparent, now, that the mechanisms of the different pressure-induced phase transitions in the three compounds of copper halides results from the three distinct phonon-softening behaviors.

ACKNOWLEDGMENTS

We would like to thank the NSERC/NRC for financial support. Calculations in this work have been done using the PWSCF package.²⁶

-
- *Permanent address: National Lab of Superhard Materials, Jilin University, ChangChun 130012, People's Republic of China.
- ¹J. C. Phillips, *Rev. Mod. Phys.* **42**, 317 (1970).
- ²V. Meisalo and M. Kalliomäki, *High Temp.-High Press.* **5**, 663 (1973).
- ³G. J. Piermarini, F. A. Mauer, S. Block, A. Jayaraman, T. H. Geballe, and G. W. Hull, Jr., *Solid State Commun.* **32**, 275 (1979).
- ⁴N. R. Serebryanaya, S. V. Popova, and A. P. Rusakov, *Sov. Phys. Solid State* **17**, 1843 (1976).
- ⁵S. Hull and D. A. Keen, *Phys. Rev. B* **50**, 5868 (1994).
- ⁶S. Baroni, S. de Gironcoli, A. Corso, and P. Giannozzi, *Rev. Mod. Phys.* **73**, 515 (2001).
- ⁷M. Buongiorno Nardelli, S. Baroni, and P. Giannozzi, *Phys. Rev. B* **51**, 8060 (1995).
- ⁸Yanming Ma, John S. Tse, and Dennis D. Klug, *Phys. Rev. B* **67**, 140301 (2003).
- ⁹S. Baroni, P. Giannozzi, and A. Testa, *Phys. Rev. Lett.* **58**, 1861 (1987); P. Giannozzi, S. de Gironcoli, P. Pavone, and S. Baroni, *Phys. Rev. B* **43**, 7231 (1991).
- ¹⁰J. P. Perdew and K. Burke, *Int. J. Quantum Chem. S* **57**, 309 (1996); J. P. Perdew, K. Burke, M. Ernzerhof, *Phys. Rev.* **77**, 3865 (1996).
- ¹¹N. Troullier and J. L. Martins, *Phys. Rev. B* **43**, 1993 (1991).
- ¹²F. D. Murnaghan, *Proc. Natl. Acad. Sci. U.S.A.* **30**, 244 (1944).
- ¹³J. W. Kremer and K. H. Weyrich, *Phys. Rev. B* **40**, 9900 (1989).
- ¹⁴R. C. Hanson, J. R. Hallberg, and C. Schwab, *Appl. Phys. Lett.* **21**, 490 (1972).
- ¹⁵S. Hoshino, Y. Fujii, J. Harada, and J. D. Axe, *J. Phys. Soc. Jpn.* **41**, 965 (1976).
- ¹⁶J. Serrano, M. Cardona, T. M. Ritter, B. A. Weinstein, A. Rubio and C. T. Lin, *Phys. Rev. B* **66**, 245202 (2002).
- ¹⁷G. Kanellis, W. Kress, and H. Bilz, *Phys. Rev. Lett.* **56**, 938 (1986); *Phys. Rev. B* **33**, 8724 (1986); **33**, 8733 (1986).
- ¹⁸B. Prevot, B. Hennion, and B. Dorner, *J. Phys. C* **10**, 3999 (1977).
- ¹⁹B. Hennion, F. Moussa, B. Prevot, C. Carabatos, and C. Schwab, *Phys. Rev. Lett.* **28**, 964 (1972).
- ²⁰B. Prevot, C. Carabatos, C. Schwab, B. Hennion, and F. Moussa, *Solid State Commun.* **13**, 1725 (1973).
- ²¹K. Persson, M. Ekman, and V. Ozoliņš, *Phys. Rev. B* **61**, 11 221 (2000).
- ²²J. Xie, S. P. Chen, J. S. Tse, D. D. Klug, Z. Li, K. Uehara, and L. G. Wang, *Phys. Rev. B* **62**, 3624 (2000).
- ²³K. Kim, V. Ozoliņš, and A. Zunger, *Phys. Rev. B* **60**, R8449 (1999).
- ²⁴P. Söderlind, O. Eriksson, J. M. Wills, and A. M. Boring, *Phys. Rev. B* **48**, 5844 (1993).
- ²⁵G. A. Samara and P. S. Peercy, in *Solid State Physics*, edited by H. Ehrenreich, F. Seitz, and D. Turnbull (Academic, New York, 1981), Vol. 36.
- ²⁶S. Baroni, A. Dal Corso, S. de Gironcoli, and P. Giannozzi, <http://www.pwscf.org>.